



Production and characterization of Ti-doped SrAl₂O₄ via volume combustion synthesis: application for dye removal

Pelin Demircivi*, Mehmet Bugdayci

Chemical and Process Engineering Department, Yalova University, Yalova 77100, Turkey, emails: pelindemircivi@gmail.com (P. Demircivi), mehmet.bugdayci@yalova.edu.tr (M. Bugdayci)

Received 21 May 2019; Accepted 3 November 2019

ABSTRACT

Titanium-doped strontium aluminate (Ti-SrAl₂O₄) composites were synthesized by volume combustion synthesis using various Ti amounts (0–20 wt.%). The composites were characterized by X-ray diffraction (XRD), scanning electron microscope and energy dispersive spectrometer analysis. XRD results showed that SrO-Sr phases, which are the residues of SrAl₂O₄ production, were eliminated after doping with Ti. The adsorption capacities of the composite samples were examined using Orange II dye in batch system for several parameters such as Ti loading amount, solution pH, contact time and temperature. Freundlich adsorption isotherm model was the best-suited model to describe the isotherm data and the maximum adsorption capacity was found to be 136.99 mg g⁻¹ at natural pH level. In acidic medium, the highest Orange II adsorption (80%) was observed, while in basic medium the adsorption of Orange II decreased to 64%. This study showed that Ti-SrAl₂O₄ could be used as an adsorbent with high adsorption capacity for removal of Orange II dye. Three-factor three-level Box–Behnken experimental design with response surface modeling was applied for statistical analysis of the experiments. Ti amount (0%–20%), solution pH (2–12) and temperature (298–318 K) were chosen as independent variables, while Orange II adsorption capacity indicated the response. Analysis of variance was used to examine the significance of independent variables and their interactions.

Keywords: Ti-doped SrAl₂O₄; Volume combustion synthesis; Orange II; Adsorption; Box–Behnken experimental design

1. Introduction

Azo dyes are used in various industrial applications such as textile, leather, pharmaceutical, plastics, etc. [1]. During the dyeing processes, 15% of the produced dye is released into the environment [2]. The synthetic dyes include complex aromatic molecules in their structures, such as benzene, toluene, xylene, etc., which make them more stable and make the biodegradation process more difficult for these molecules [3]. Orange II is one of the synthetic dyes that is used in various industrial applications. Having carcinogenic and mutagenic effects, these dyes have hazardous effects on

the ecosystem. Therefore, removal of Orange II from wastewaters is one of the important problems from the environmental point of view.

Possible elimination processes of Orange II by adsorption [1,4], oxidation [5], chemical degradation [6,7] and photocatalysis [8] were studied and added to the literature. Zeolite, chitosan and biomass are some of the materials that were used for dye adsorption [7–10]. Jin et al. [11] studied Orange II dye adsorption using hexadecyltrimethylammonium-bromide (HDTMA) modified zeolite, which was used to change the surface charge from negative to positive. Adsorption capacity of HDTMA modified zeolite reached 38.96 mg g⁻¹, while

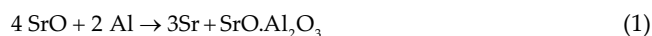
* Corresponding author.

natural zeolite reached 8.13 mg g^{-1} . Orange II dye adsorption occurred according to Freundlich isotherm model and the reaction kinetics was found to be pseudo-second order [11]. Kong et al. [12] found that activated carbon derived from sawdust had an important adsorption capacity for Orange II dye molecule. Depending on the mass ratios between calcium carbonate and sawdust, the highest adsorption capacity was found to be 389 mg g^{-1} due to the increasing surface area and total pore volume [12]. Qin et al. [13] investigated the adsorption capacity of trimethylchlorosilane (TMCS) and Al_{13} intercalated montmorillonite for Orange II dye adsorption. Removal of the dye was achieved at 98.7%, while the initial concentration of the dye solution was $1,000 \text{ mg L}^{-1}$. It was showed that the Langmuiran adsorption with a maximum adsorption capacity of 118.6 mg g^{-1} [13].

Nowadays, the use of composite materials for the adsorption process has attracted much attention. SrAl_2O_4 is one of the composite materials that can be used for the adsorption of pollutants in environment. The strontium and its compounds, which are elements of group IIA of periodic table, are produced from celestine ore and its compounds are produced from barite ore. World barite base reserves (economic reserve + reserve that may be future economic) are around 500 million tons [14,15]. Due to high amount of reserves, it is important to find areas of usage (such as environmental usage) for Sr and its compounds effectively.

García et al. [16] investigated the photocatalytic degradation of methylene blue and congo red under ultraviolet light and solar irradiation using bismuth-doped SrAl_2O_4 which was produced via combustion synthesis method. Combustion method is a kind of self propagating high temperature synthesis (SHS) and it was used in this study. SHS is one of the important methods to synthesize advanced materials such as ceramics, abrasives, cutting tools, polishing powders, resistive heating elements, shape-memory alloys, high-temperature structural alloys, master alloys and oxides [17]. Nakauchi et al. [18] synthesized Nd-doped SrAl_2O_4 crystals by a floating zone (FZ) method using an FZ furnace ($1,500^\circ\text{C}$ 6 h) and characterized its optical and scintillation properties.

Main strontium production route is reduction of its oxide with aluminum. The reduction took place according to Eq. (1) and reaction residues are SrAl_2O_4 under vacuum [19].



Bugdayci et al. [20] investigated the related process thermodynamically. SrAl_2O_4 phase was observed over 210°C under vacuum using this process. They also emphasized that, during aluminothermic Sr reduction, SrO converts $\text{Sr}_{(g)}$ at $1,100^\circ\text{C}$ [20]. Therefore, in order to produce metallic Sr, the system needs high temperature (min $1,100^\circ\text{C}$) and vacuum conditions. Otherwise, the reaction proceeds according to Eq. (2) and SrO is converted to SrAl_2O_4 .



In this way, production of SrAl_2O_4 is possible without vacuum condition. Prior to the start of the experiments, thermodynamic simulations were done via FactSage 7.1 program.

Fig. 1 presents possible phases of SrO–Al reaction. According to Fig. 1, it is clear that the Al_2Sr phase is formed over 195°C . Before reaching this temperature, there is not any reaction between Al and SrO. These phases are stable until 660°C . Over 660°C , the amount of Al_2Sr is reduced and SrO converts to SrAl_2O_4 . Over 700°C , the reaction proceeds to form about 260 g of SrAl_2O_4 and 20 g of Al_2Sr [21].

The main purpose of this study was not only the production of SrAl_2O_4 , but also the production of Ti-doped SrAl_2O_4 . In order to understand Ti-doped SrOAl_2O_3 production, probable phases were calculated and presented in Fig. 2. According to Fig. 2, behaviors of Al and SrO show similarities with Fig. 1 until 610°C . In addition, TiO does not react until 610°C . Over this temperature, Ti reacts with Al and according to this reaction TiAl phase is detected. In resemblance to Fig. 1, the SrAl_2O_4 phase occurs after 660°C with the new $(\text{SrO})_2\text{TiO}_2$ phase. It is clearly understood from Fig. 2 over 660°C that, SrAl_2O_4 , TiAl and $(\text{SrO})_2\text{TiO}_2$ are stable phases of the reaction.

In this study, a novel adsorbent, Ti-SrAl₂O₄, was synthesized and characterized for the first time. The adsorption capacity of Ti-SrAl₂O₄ was experimentally studied and determined by using Orange II dye. Batch studies were conducted to investigate the adsorption capacity of the composites. The effects of experimental conditions such as Ti amount, solution pH, contact time and temperature on adsorption were studied and possible adsorption mechanism is presented. To identify the effects of independent variables (Ti amount, solution pH and temperature) on adsorption capacity of Ti-SrAl₂O₄ three-factor three-level Box–Behnken experimental design was applied.

2. Materials and methods

2.1. Preparation of Ti-loaded SrAl₂O₄ composites

In the experiments, Alfa Aesar (United Kingdom) technical grade SrO was used as strontium source and its properties are given in Table 1. Al powder was used as reductant which has 99.02% purity and lower than 150 micron grain size. Chemical analyses of Al are given in Table 2. High grade,

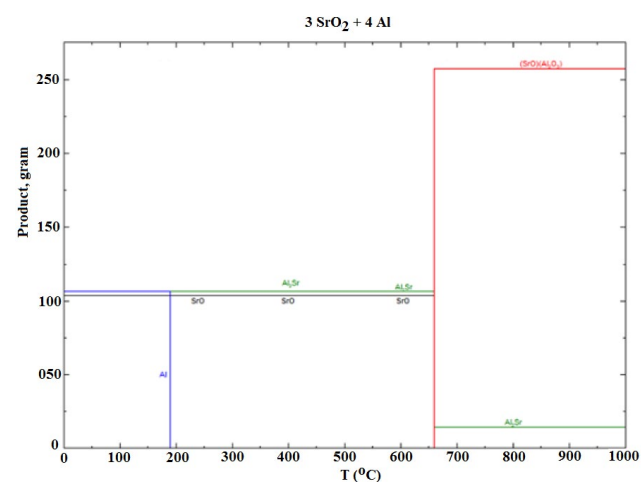


Fig. 1. SrAl_2O_4 production simulation with ranging temperature and Al addition [18].

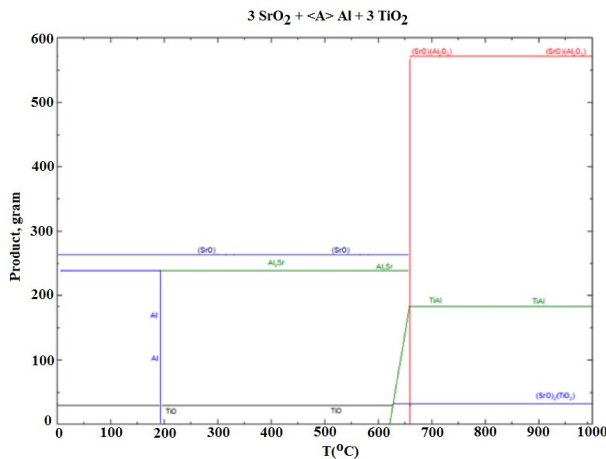


Fig. 2. Ti-doped SrAl_2O_4 production simulation with ranging temperature and Al addition [18].

Table 1
SrO-TiO₂ physical and thermal properties

Compound	SrO	TiO ₂
T_{melt} (°C)	2,430	1,843
T_{boil} (°C)	3,000	2,972
Density (g/cm ³)	4.70	4.23
Weight (g)	103.62	79.93
Form	–100 mesh	–100 mesh

Table 2
Chemical analysis of Al

Si	–
Fe	0.84
Al	99.02
Ca	–
Mg	0.01

TiO₂ (Merck, 99.00%, USA) was used as Ti Source and also its properties are given in Table 1.

Production of SrAl_2O_4 was examined in the first experiment. 100% stoichiometric (stoc.) SrO-Al mixture was weighted and dried in a drying oven at 105°C for 60 min. After the drying process, the ingredients were mixed with each other in a turbula mixer for 15 min. These mixtures were loaded in a chamotte crucible ($\text{Al}_2\text{O}_3\cdot\text{SiO}_2$) and then placed in the ash furnace. Fig. 1 shows that SrAl_2O_4 production is possible above 660°C. After the furnace reached to 660°C, the mixture remained in the furnace for 1 h. Finally crucibles were taken from the furnace and examined.

After the SrAl_2O_4 production process explained above, a new set of experiments was performed to investigate the effects of Ti addition. TiO₂-Al (100% stoc.) mixture was added to SrO-Al mixture so that the content of TiO₂-Al mixture was 5%, 10%, 15% and 20% by weight in the resulting mixture, respectively. In the light of thermodynamic

calculations, the same procedure as the first experiment was applied. According to Fig. 2 all reactions took place above 660°C.

2.2. Characterization of the composites

Characterization of $\text{TiSrAl}_2\text{O}_4$ powders was done by SEM and X-ray diffraction (XRD) techniques. XRD investigations of the Ti-SrAl₂O₄ samples were performed by using a Bruker™ D8 Advanced Series powder diffractometer (Germany) (operated at 35 kV and 40 mA) with $\text{CuK}\alpha$ ($k = 1.5406 \text{ \AA}$) radiation at 2 h range of 10°–90° using a step size of 0.02° and a rate of 2°/min. Ti-SrAl₂O₄ powders were characterized by using X'pert High Score software coupled with XRD with five measurements conducted on each powder sample. Microstructures of the Ti-SrAl₂O₄ samples were observed using a JEOL JCM-6000Plus NeoScope (France) scanning electron microscope (SEM) operated at 15 kV, which is equipped with an energy dispersive spectrometer (EDS).

2.3. Adsorption studies

Batch adsorption experiments were performed by shaking 25 mL of Orange II solution (100 mg L⁻¹) in a water bath orbital shaker at 140 rpm, 298 K for 24 h. The effect of pH on Orange II adsorption was studied at different pH levels (2.0–12.0). The pH levels of Orange II solutions were adjusted by the addition of HCl and NaOH solutions. Thermodynamic studies were conducted at 298, 308 and 318 K using 100 mg L⁻¹ initial Orange II concentration.

The equilibrium studies were conducted at different solid/liquid ratios between 0.08 and 7.0 g L⁻¹ for 24 h at the neutral pH value and 298 K with various loading amounts of titanium ranging from 0% to 20%. The equilibrium Orange II concentrations were analyzed by UV-Vis spectrophotometer at 485 nm. Batch adsorption experiments were conducted in triplicate and arithmetically averaged results were used to fit adsorption curves. The amount of Orange II adsorbed by Ti-SrAl₂O₄ samples was calculated by using Eq. (3) as follows:

$$q_e = \frac{(C_i - C_e) \times V}{m} \quad (3)$$

where q_e is the Orange II adsorption capacity (mg g⁻¹), V is the solution volume (L), m is the adsorbent dosage (g), C_i and C_e are the initial and equilibrium concentration of Orange II (mg L⁻¹), respectively.

The kinetic adsorption experiments performed by mixing Orange II solution (20 mg L⁻¹) at natural pH with Ti-SrAl₂O₄-20 samples in polyethylene bottles at 298 K using 3.0 g/L solid/liquid ratio. At given time intervals, aliquots (4 mL) were withdrawn and filtered through 0.45 μm syringe filter and equilibrium Orange II concentrations were measured.

2.4. Box-Behnken experimental design

To investigate the effective parameters on Orange II adsorption capacity three-factor three-level Box-Behnken experimental design was studied by combining response surface modeling. Box-Behnken design reduces the number

of experiments to investigate the effects of parameters. Three factors considered as independent variables Ti amount (x_1), solution pH (x_2) and temperature (x_3). The high, low and central levels were represented as +1, -1 and 0 as listed in Table 3. The analysis of variance (ANOVA) was used to analyze the statistical significance of independent variables. Design-Expert Software (Ver. 7.0, Stat-Ease, Minneapolis, USA) software package was used for regression and graphical analyses. Quadratic approximation of Box–Behnken model was evaluated with 95% confidence limits ($\alpha = 0.05$).

3. Results and discussion

3.1. Characterization of the samples

First SrAl_2O_4 production parameters were investigated in the experiments. Prior to the experiments, minimum reaction temperature and probable phases were calculated via FactSage program. According to the results, minimum reaction temperature was calculated as 660°C for SrAl_2O_4 production. Afterwards, Ti-doped experiments were simulated and it was determined that the desired products can be obtained at the same temperature. All the composite samples were characterized by XRD technique; Fig. 3 displays representative XRD patterns of samples. In the experiment of SrAl_2O_4 production, desired phase was obtained but some unreacted SrO and with Al_2O_3 reduced Sr phases were detected. Thereafter, Ti-doped experiments were performed and all SrO-Sr phases were eliminated due to the addition of titanium, which promoted the formation of Sr_2TiO_4 and Al_2Ti phases. On the other hand, a very limited amount of these phases were detected at 5% and 10% Ti-doped experiments. At 15% and 20% Ti-doped experiments the amount of Sr_2TiO_4 (B_{XRDgrap}) and Al_2Ti (C_{XRDgrap}) phases increased. In these experiments, very low amounts of reduced Ti (D_{XRDgrap}) phases were observed in addition to the other phases. It was clearly seen that Al_2O_3 phases were obtained in all of the experiments but the amount of this phase is decreased with increasing amount of Ti added.

Figs. 4a–c consist of the respective representative SEM images of the Ti- SrAl_2O_4 (0%–20%) powders. Fig. 4 illustrates the EDS spectral analysis graphs taken from the specified regions on Figs. 4a–c. According to SEM images, Ti addition increases to surface area of the powder grains, because the porosity rate of the visuals decreases from (a) to (c). SEM images also showed that increasing Ti amount provide smoother surface when compared with the SrAl_2O_4 surface. EDS spectral analyses of images show that the amount of Ti increases from 1.4% (by weight) to 4.5% (by weight) with 10% Ti addition.

3.2. Effect of titanium amount on Orange II adsorption

Adsorption capacities of various synthesized Ti- SrAl_2O_4 (0–20%) composites were compared for Orange II adsorption by conducting experiments with 25 mL 100 mg L⁻¹ Orange II solution at 298 K. As presented in Fig. 5, the Orange II adsorption capacity significantly increased from 43 mg g⁻¹ (Ti- SrAl_2O_4 -0) to 140 mg g⁻¹ (Ti- SrAl_2O_4 -20). Titanium is a cation (Ti^{4+}) and makes the surface positively charged, which causes an increase in adsorption. Increasing in

Table 3
Levels of independent variables and experimental range

Independent variables	Symbol	Levels		
		-1	0	1
Ti amount, %	x_1	0	10	20
pH	x_2	2	6.5	11
Temperature, K	x_3	25	35	45

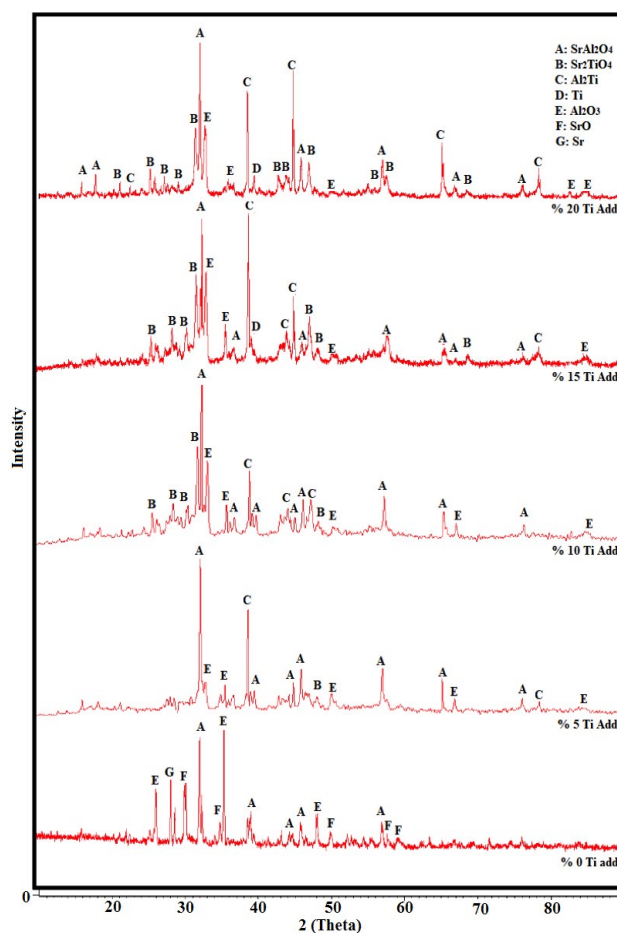


Fig. 3. XRD graphic of SrAl_2O_4 and Ti-doped SrAl_2O_4 products.

adsorption capacity is a result of electrostatic attractions between positively charged surface and Orange II anion. Therefore, Ti- SrAl_2O_4 -20 composite was used for the further experiments.

3.3. Effect of pH on Orange II adsorption

Solution pH is an important parameter due to ionization of the adsorbate and due to the change of surface properties of the adsorbent. Therefore, the effect of solution pH on Orange II adsorption was investigated using 100 mg L⁻¹ Orange II solution at different pH levels (2–12). As illustrated in Fig. 6, the highest Orange II adsorption capacity of Ti- SrAl_2O_4 -20 was achieved between pH 2 and 6 (80%,

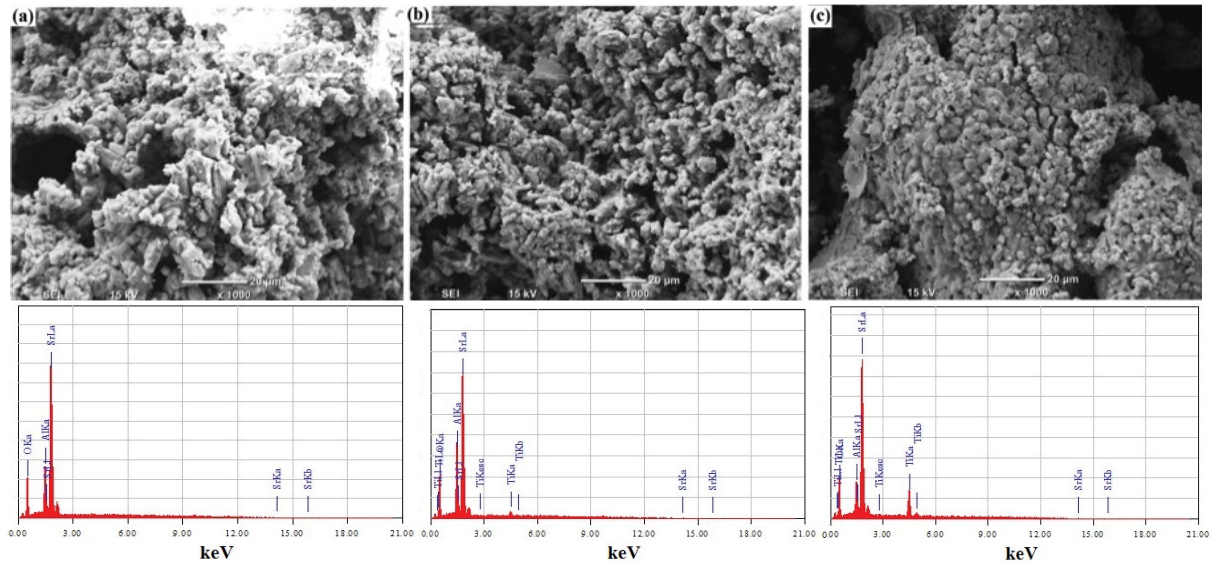


Fig. 4. SEM images and EDS analyses of SrAl_2O_4 and Ti-doped SrAl_2O_4 products, ((a) %0 Ti add., (b) %10 Ti add., (c) %20 Ti add.).

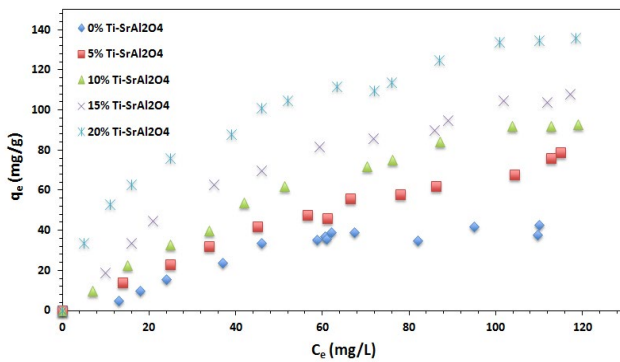


Fig. 5. Effect of titanium amount on AOII adsorption.

30 mg g^{-1}) due to the electrostatic attractions between the positively charged surface and the Orange II anions. In neutral medium, a slight decrease (64% , 32 mg g^{-1}) in adsorption was observed because of the competition between the negatively charged OH^- ions and the Orange II anions. Kong et al. [12] studied the adsorption of Orange II on activated carbon, which was produced from sawdust. They also found the maximum adsorption capacity at pH levels lower than 5, which was a result of electrostatic attractions between the dye molecules and the positively charged surface [12].

3.3. Adsorption isotherms

Adsorption studies were performed with a number of Ti- SrAl_2O_4 composites with different titanium loading levels (0–20%) by shaking with $25 \text{ mL } 100 \text{ mg L}^{-1}$ Orange II solution at 140 rpm and 298 K using 3.0 g L^{-1} solid/liquid ratio. In order to investigate the adsorption characteristics of Ti- SrAl_2O_4 composites, Langmuir, Freundlich and Dubinin–Radushkevich (D-R) isotherm models were used to analyze the adsorption data.

Langmuir isotherm model assumes that the adsorption occurs on homogenous surface sites on the adsorbent and

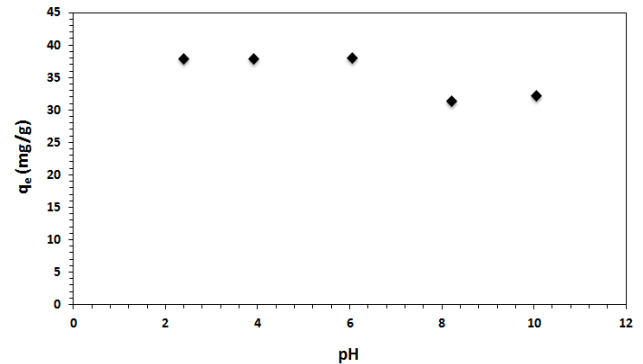


Fig. 6. Effect of pH on AOII adsorption.

monolayer coverage occurs on the same adsorption energy sites [22,23]. The linear form of the Langmuir isotherm equation is given in Eq. (4);

$$\frac{C_e}{q_e} = \frac{1}{Qb} + \frac{C_e}{Q} \quad (4)$$

where q_e is the amount of Orange II adsorbed at equilibrium (mg g^{-1}), C_e is the equilibrium Orange II concentration in the solution (mg L^{-1}), Q is the monolayer capacity of the adsorbent (mg g^{-1}) and b is the Langmuir adsorption constant (L mg^{-1}).

Freundlich isotherm model takes place on heterogeneous surface sites with non-uniform distribution of sorption heat. Multilayer coverage occurs on heterogeneous surface sites [24]. The linear form of the Freundlich isotherm equation is given in Eq. (5);

$$\log q_e = \log K_F + \frac{1}{n} \log C_e \quad (5)$$

where q_e is the amount of Orange II adsorbed at equilibrium (mg g^{-1}), C_e is the equilibrium Orange II concentration in the

solution (mg L⁻¹), K_f is Freundlich constant related to the adsorption capacity (L g⁻¹) and n is the Freundlich constant related to adsorption intensity.

D–R model is often used to distinguish physical and chemical adsorption mechanisms [25]. The linear form of the D–R isotherm equation is given in Eq. (6):

$$\ln q_e = \ln q_m - B\epsilon^2 \quad (6)$$

where q_e is the amount of Orange II adsorbed at equilibrium (mg g⁻¹), q_m is the maximum adsorption capacity of the adsorbent (mg g⁻¹), B is the constant about mean free energy of the adsorption (mmol² kJ⁻²), ϵ is the Polanyi potential (J mmol⁻¹). ϵ is calculated from the following equation:

$$\epsilon = RT \ln \left(1 + \frac{1}{C_e} \right) \quad (7)$$

The mean free energy (E) is calculated from the following equation:

$$E = \frac{1}{(2B)^{1/2}} \quad (8)$$

The parameters obtained from the isotherm models were given in Table 4.

According to the correlation coefficients (R^2) given in Table 4, Freundlich isotherm is the best-suited model to describe the experimental data of Orange II adsorption (Fig. 7). This result indicates that the multilayer adsorption of Orange II occurred on heterogeneous surface sites of Ti-SrAl₂O₄-20. The Pearson’s correlation coefficients were also the evidence of Freundlich isotherm model best described the adsorption process. The correlation coefficients were found to be 0.98, 0.99 and 0.75 for Langmuir, Freundlich and Dubinin–Radushkevich isotherm models, respectively. Adsorption capacities of Orange II on Ti-SrAl₂O₄-0 and Ti-SrAl₂O₄-20 were found as 39 and 134 mg g⁻¹, respectively. Increasing the adsorbent dosage from 0.002 to 0.075 g increased the adsorption percentage from 8% to 96%. This result was due to the enhancing of the available adsorption sites on the adsorbent. Adsorbent dosages beyond 0.075 g did not show a significant effect on the adsorption of Orange II because the equilibrium between solid and liquid phases was reached at this dosage. Therefore, the adsorbent dosage of 0.075 g was used for the further experiments. Jin et al. [11] investigated the Orange II adsorption on surfactant-coated zeolite. According to the results, Freundlich model was found to fit better to the adsorption data of Orange II dye [11].

3.4. Adsorption kinetics

To investigate the effect of contact time experiments with 100 mg L⁻¹ Orange II solution and Ti-SrAl₂O₄-20 composite using 3.0 g L⁻¹ solid/liquid ratio were conducted. The equilibrium time was found to be 22 h, which indicates that all of the active sites on the composite surface were completely occupied with Orange II ions after 22 h (Fig. 8). The adsorbed amount of Orange II was found to be 103 mg g⁻¹ at the equilibrium time.

The kinetic parameters were evaluated for the adsorption of Orange II onto the Zr(IV)-CS-PT composite using the pseudo-first-order, the pseudo-second-order and the intra-particle diffusion models. The pseudo-first-order kinetic model is also known as Lagergren kinetic model and expresses the kinetic behavior of the adsorption reactions. The pseudo-first order rate equation of Lagergren is given in Eq. (9);

$$\log(q_e - q_t) = \log q_e - \frac{k_1}{2.303} t \quad (9)$$

where q_e and q_t are the amounts of adsorbed Orange II at equilibrium and at time t (mg g⁻¹) and k_1 is the pseudo-first-order rate constant (min⁻¹).

The pseudo-second-order rate equation is given in Eq. (10):

$$\frac{t}{q_t} = \frac{1}{k_2 q_e^2} + \frac{1}{q_e} t \quad (10)$$

where q_e and q_t are the amounts of adsorbed Orange II at equilibrium and time t (mg g⁻¹) and k_2 is the pseudo-second-order rate constant (g mg⁻¹ min⁻¹).

The intra-particle diffusion model is given in Eq. (11):

$$q_t = k_{int} t^{1/2} + c \quad (11)$$

where q_t is the amount of adsorbed Orange II at time t (mg g⁻¹), k_{int} is the intra-particle diffusion rate constant (mg g⁻¹ min^{-1/2}), t is the time (min) and c is the intercept (mg g⁻¹).

The calculated kinetic parameters are given in Table 5. According to the correlation coefficients (R^2), the pseudo-second order kinetic model was found to be the best model for the kinetic data. The adsorption of Orange II on Ti-SrAl₂O₄-20 occurs by sharing valence forces or exchange of electrons between adsorbent and adsorbate [26].

3.5. Adsorption thermodynamics

Table 6 indicates that the adsorption capacity of Ti-SrAl₂O₄-20 increased with increasing temperature.

Table 4
Isotherm parameters of AOII adsorption on Ti-SrAl₂O₄

Adsorbent	Langmuir isotherm			Freundlich isotherm			Dubinin–Radushkevich isotherm		
	Q_m (mg/g)	b	R^2	K_f (mg/g)	n	R^2	q_m (mg/g)	B (mmol ² /kJ ²)	R^2
0% Ti-SrAl ₂ O ₄	107.53	0.029	0.91	1.730	13.881	0.94	39.173	51.705	0.84
20% Ti-SrAl ₂ O ₄	136.99	0.078	0.97	18.38	2.325	0.99	105.636	6.305	0.70

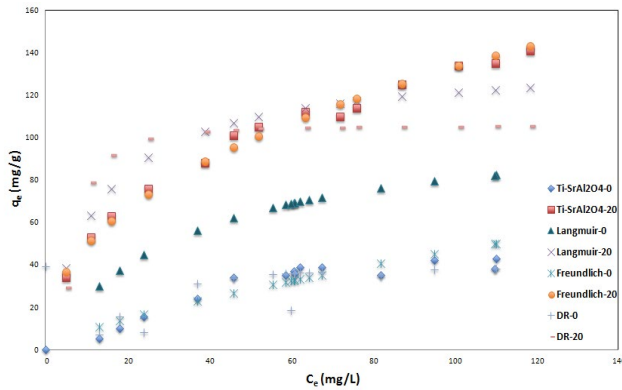


Fig. 7. Comparison of calculated and experimental data of isotherm models.

Table 5
Kinetic data of AOII adsorption

Pseudo-first order model			Pseudo-second order model			Intra-particle diffusion model		
k_1 (L/min)	q_e (mg/g)	R^2	k_2 (g/mg min)	q_e (mg/g)	R^2	k_{int} (mg/g min ^{1/2})	c	R^2
0.0016	118.141	0.89	0.0055	139.876	0.98	3.172	21.913	0.96

Table 6
Thermodynamic data of AOII adsorption

C_0 (mg/L)	T (K)	ΔH (kJ/mol)	ΔG (kJ/mol)	ΔS (J/mol K)
	298		-1.127	
100	308	15.73	-1.431	0.056
	318		-2.121	

Thermodynamic parameters such as Gibbs free energy (ΔG°), the change in enthalpy (ΔH°) and entropy (ΔS°) were calculated for a solution with 100 mg L⁻¹ Orange II concentration in order to evaluate the thermodynamic feasibility of the adsorption process. The positive value of ΔH° (15.73 kJ mol⁻¹) confirmed the endothermic nature of the adsorption process, while the negative ΔG° values indicate that the Orange II adsorption on Ti-SrAl₂O₄-20 is thermodynamically spontaneous and feasible. The positive value of ΔS° suggested an increase in the randomness at solid/liquid interface; however the low value of ΔS° indicates that there are no significant changes in entropy during the adsorption process [27].

3.6. Statistical analysis

Experimental design was used to determine the most effective parameters on the response with less number of experiments. For our three-factor three-level experimental design, 17 runs were carried out including five center points. To identify the contribution of independent variables and their significance, a polynomial regression equation was developed. Table 7 represents the responses (q_e) of 17 runs and based on the results Orange II adsorption capacity (q_e) was improved from 20.0 to 37.5 mg g⁻¹.

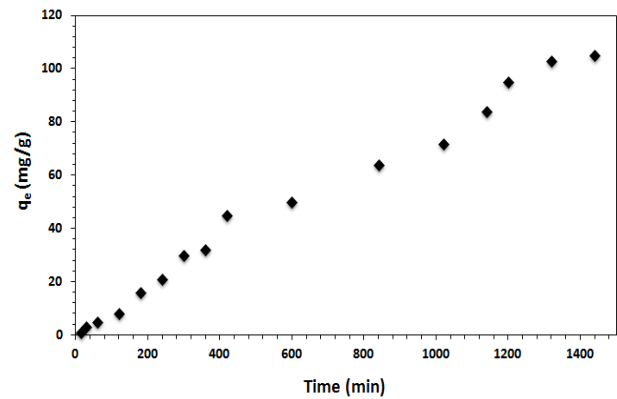


Fig. 8. Effect of contact time on AOII adsorption.

The model for Orange II adsorption suggested a quadratic model. The interaction of independent variables and the response was performed by regression analysis and the adsorption of Orange II was found as:

$$q_e = 20.00 + 3.13x_1 - 0.75x_2 - 0.62x_3 - 0.25x_1x_2 + 1.50x_1x_3 - 0.75x_2x_3 + 5.75x_1^2 + 3.00x_2^2 + 7.75x_3^2 \quad (12)$$

The correlation coefficient (R^2) of the given model was obtained 0.94, which indicated the good correlation between the experimental and predicted response values.

The results of the ANOVA model are given in Table 8. F -value of the model was obtained as 8.32, which implies that the model is significant. The significance of the parameters was evaluated with probability values (p -values). p -value less than 0.05 implies that the effect is significant.

The response surface plots were evaluated to identify the relation between the independent variables and response. To examine the response surface models, one independent variable was kept constant while plotting the surface model as a function of the other independent variables.

4. Conclusion

In this work, Ti-SrAl₂O₄ was prepared via volume combustion synthesis and characterized for Orange II adsorption. The XRD analyses proved the formation of Ti-SrAl₂O₄ composites. Different amounts of Ti were loaded (0%–20%) into SrAl₂O₄ structure. It was found that Ti-SrAl₂O₄-20 showed the highest adsorption capacity. According to the pH experiments, the Orange II adsorption was slightly decreased in basic medium due to the electrostatic repulsion forces between the negatively charged surface and the Orange II anions. The presence of OH ions in the solution is another

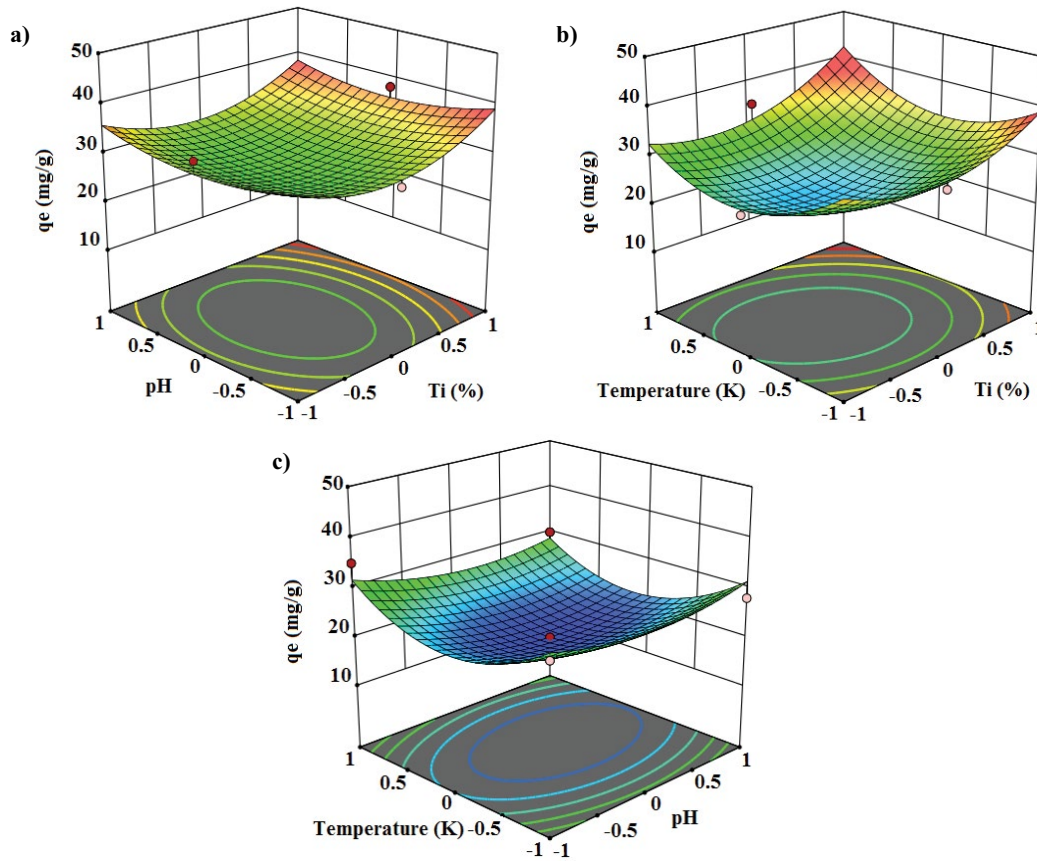


Fig. 9. 3D response surface diagrams showing the effects of (a) Ti amount (%) and pH at constant temperature; (b) Ti amount (%) and temperature at constant pH; (c) pH and temperature at constant Ti amount (%) on the adsorption capacity of Ti-doped SrAl₂O₄.

Table 7
Codes of independent variables, observed and predicted sorption capacities

Run	Independent variables						Adsorption capacity (mg/g)	
	Ti %, x_1		pH, x_2		Temperature, x_3		Observed	Predicted
	Coded	Actual	Coded	Actual	Coded	Actual		
1	0	10	-1	2	1	45	35.00	31.62
2	0	10	-1	2	-1	25	30.00	31.37
3	0	10	1	10	-1	25	28.00	31.37
4	1	20	1	10	0	35	32.00	30.87
5	0	10	1	10	1	45	30.00	28.62
6	-1	0	1	10	0	35	26.00	25.12
7	0	10	0	5	0	35	20.00	20.00
8	-1	0	-1	2	0	35	25.00	26.12
9	0	10	0	5	0	35	20.00	20.00
10	1	20	0	5	-1	25	38.00	35.75
11	0	10	0	5	0	35	20.00	20.00
12	-1	0	0	5	-1	25	35.00	32.50
13	0	10	0	5	0	35	20.00	20.00
14	1	20	-1	2	0	35	32.00	32.87
15	1	20	0	5	1	45	35.00	37.50
16	-1	0	0	5	1	45	26.00	28.25
17	0	10	0	5	0	35	20.00	20.00

Table 8
ANOVA of second-order polynomial equation

Factors	Sum of squares	df	Mean square	F-value	p value
Model	569.81	9	63.31	8.32	0.0054
x_1	78.13	1	78.13	10.27	0.0150
x_2	4.5	1	4.5	0.5915	0.4670
x_3	3.13	1	3.13	0.4108	0.5420
x_1x_2	0.2500	1	0.2500	0.0329	0.8613
x_1x_3	9.00	1	9.00	1.18	0.3128
x_2x_3	2.25	1	2.25	0.2958	0.6034
x_{12}	139.21	1	139.21	18.30	0.0037
x_{22}	37.89	1	37.89	4.98	0.0608
x_{32}	252.89	1	252.89	33.24	0.0007
Lack of fit	53.25	3	17.75		
Pure error	0.0000	4	0.0000		
Total SS	623.06	16			

major cause of this decrease in adsorption. From the thermodynamic data, it was found that an increase in the temperature resulted in an increase in the adsorption capacity and the adsorption behavior was spontaneous and endothermic. Comparing the adsorption isotherm models, the Freundlich isotherm model showed a good correlation with the experimental data. The results showed that Ti-SrAl₂O₄ composite could be used for dye adsorption with a high adsorption capacity. To scale up the adsorption process, column experiments will be studied in further.

References

- [1] L. Zhang, Z. Cheng, X. Guo, X. Jiang, R. Liu, Process optimization, kinetics and equilibrium of orange G and acid orange 7 adsorptions onto chitosan/surfactant, *J. Mol. Liq.*, 197 (2014) 353–367.
- [2] A. Houas, H. Lachheb, M. Ksibi, E. Elaloui, C. Guillard, J.M. Herrmann, Photocatalytic degradation pathway of methylene blue in water, *Appl. Catal., B*, 31 (2001) 145–157.
- [3] F. Shakeel, N. Haq, F.K. Alanazi, I.A. Alsarra, Box-Behnken statistical design for removal of methylene blue from aqueous solution using sodium dodecyl sulfate self-microemulsifying systems, *Ind. Eng. Chem. Res.*, 53 (2014) 1179–1188.
- [4] S. Mondal, Methods of dye removal from dye house effluent-an overview, *Environ. Eng. Sci.*, 25 (2008) 383–396.
- [5] V.K. Gupta, Application of low-cost adsorbents for dye removal-a review, *J. Environ. Manage.*, 90 (2009) 2313–2342.
- [6] A.K. Verma, R.R. Dash, P. Bhunia, A review on chemical coagulation/flocculation technologies for removal of colour from textile wastewaters, *J. Environ. Manage.*, 93 (2012) 154–168.
- [7] G. Crini, Non-conventional low-cost adsorbents for dye removal-a review, *Bioresour. Technol.*, 97 (2006) 1061–1085.
- [8] A. Mittal, J. Mittal, A. Malviy, V.K. Gupta, Removal and recovery of chrysoidine Y from aqueous solutions by waste materials, *J. Colloid Interface Sci.*, 344 (2010) 497–507.
- [9] N.M. Mahmoodi, R. Salehi, M. Arami, H. Bahrami, Dye removal from colored textile wastewater using chitosan in binary systems, *Desalination*, 267 (2011) 64–72.
- [10] C.Y. Tan, M. Li, Y.M. Lin, X.Q. Lu, Z.L. Chen, Biosorption of basic orange from aqueous solution onto dried *A. Filiculoides* biomass: equilibrium, kinetic and FTIR studies, *Desalination*, 266 (2011) 56–62.
- [11] X. Jin, B. Yu, Z. Chen, J.M. Arocena, R.W. Thring, Adsorption of Orange II dye in aqueous solution onto surfactant-coated zeolite: characterization, kinetic and thermodynamic studies, *J. Colloid Interface Sci.*, 435 (2014) 15–20.
- [12] L. Kong, M. Su, Y. Peng, L. Hau, J. Liu, H. Li, Z. Diao, K. Shih, Y. Xiong, D. Chen, Producing sawdust derived activated carbon by co-calcinations with limestone for enhanced Acid Orange II adsorption, *J. Clean. Prod.*, 168 (2017) 22–29.
- [13] Z. Qin, P. Yuan, S. Yang, D. Liu, H. He, J. Zhu, Silylation of Al13-intercalated montmorillonite with trimethylchlorosilane and their adsorption for Orange II, *Appl. Clay Sci.*, 99 (2014) 229–236.
- [14] İ. Demirkaya, E. Acma, Evaluation methods and usage possibilities of celestite and baryt concentrates, *Metallurji*, 24 (2017) 1–13.
- [15] Ullmans, Enclopadie, Band 22,4, Auflage, 1982, pp. 287–291.
- [16] C.R. García, J. Oliva, A. Arroyo, M.A. Garcia-Lobato, C. Gomez-Soli, L.A. Diaz Torres, Photocatalytic activity of bismuth doped SrAl₂O₄ ceramic powders, *J. Photochem. Photobiol., A*, 351 (2018) 245–252.
- [17] A. Turan, M. Bugdayci, O. Yucel, Self-propagating high temperature synthesis of TiB₂, *High Temp. Mater. Proc.*, 34 (2015) 185–193.
- [18] D. Nakauchi, G. Okada, M. Koshimizu, T. Yanagida, Optical and scintillation properties of Nd-doped SrAl₂O₄ crystals, *J. Rare Earth*, 34 (2016) 757–762.
- [19] Ullmann Encyclopedia, Strontium and Strontium Compounds Wiley-VCH Verlag GmbH & Co. KGaA, Weinheim, 2005, pp. 1–8.
- [20] M. Bugdayci, K.C. Tasyurek, O. Yucel, Thermodynamic Modelling of Magnesium-Oxide, Calcium-Oxide and Strontium-Oxide Reduction Systems Via Pidgeon Process, TMS 2018: 9th International Symposium on High-Temperature Metallurgical Processing, 2018, pp. 81–89.
- [21] FactSage 7.1 Database.
- [22] C.K. Lim, H.H. Bay, C.H. Neoh, A. Aris, Z.A. Majid, Z. Ibrahim, Application of zeolite-activated carbon macrocomposite for the adsorption of Acid Orange 7: isotherm, kinetic and thermodynamic studies, *Environ. Sci. Pollut. Res.*, 20 (2013) 7243–7255.
- [23] M.Q. Jiang, Q.P. Wang, X.Y. Jin, Z.L. Chen, Removal of Pb(II) from aqueous solution using modified and unmodified kaolinite clay, *J. Hazard. Mater.*, 170 (2009) 332–339.
- [24] C. Ng, J.N. Losso, W.E. Marshall, R.M. Rao, Freundlich adsorption isotherms of agricultural by-product-based powdered activated carbons in a geosmin-water system, *Bioresour. Technol.*, 85 (2002) 131–135.

- [25] W.J. Thomas, B. Crittenden, *Adsorption Technology & Design*, 1st ed. Elsevier Science & Technology Books, 1998.
- [26] Q. Liu, P. Hu, J. Wang, L. Zhang, R. Huang, Phosphate adsorption from aqueous solutions by Zirconium (IV) loaded cross-linked chitosan particles, *J. Taiwan Inst. Chem. Eng.*, 59 (2016) 311–319.
- [27] R. Han, J. Zhang, P. Han, Y. Wang, Z. Zhao, M. Tang, Study of equilibrium, kinetic and thermodynamic parameters about methylene blue adsorption onto natural zeolite, *Chem. Eng. J.*, 145 (2009) 496–504.